

Measurement of Spin Correlation in Proton-Proton Scattering at 400 and 450 MeV*

E. ENGELS, JR.,† T. BOWEN,‡ J. W. CRONIN, AND R. L. McILWAIN§
Princeton University, Princeton, New Jersey

AND

LEE G. PONDROM
Columbia University, New York, New York
 (Received 17 September 1962)

The spin correlation coefficients C_{nn} and C_{KP} for proton-proton scattering have been measured at 400 MeV (60° and 90° in the center-of-mass system) and at 450 MeV (90° in the center-of-mass system) using spark chambers containing carbon plates as the polarization analyzers. At 400 MeV, the results are: $C_{nn}(90^\circ) = 0.60 \pm 0.09$, $C_{KP}(90^\circ) = 0.32 \pm 0.09$, $C_{nn}(60^\circ) = 0.82 \pm 0.47$, and $C_{KP}(60^\circ) = 0.60 \pm 0.46$. At 450 MeV, the results are: $C_{nn}(90^\circ) = 0.70 \pm 0.15$ and $C_{KP}(90^\circ) = 0.37 \pm 0.14$. The results of the 400-MeV measurements are consistent with predicted values for these coefficients obtained by extrapolating the proton-proton phase shifts from lower energies. Phase-shift extrapolations to 450 MeV are not as yet available.

I. INTRODUCTION

THIS paper reports the first in a series of experiments which apply the spark chamber technique to the measurement of the nucleon-nucleon scattering matrix. The review article by MacGregor, Moravcsik, and Stapp gives an excellent introduction to the subject through mid-1960.¹ Since that time energy-dependent phase-shift fits have been attempted by two different groups using the extensive data between zero and 310 MeV.^{2,3} These fits allow an extrapolation to be made to 400 MeV. In the present experiment the correlation coefficients C_{nn} and C_{KP} in p - p scattering at 90° and 60° in the center of mass at 400-MeV bombarding energy and at 90° in the center of mass at 450 MeV have been measured.

The coordinate system used to define the coefficients is shown in Fig. 1(a). \mathbf{k} and \mathbf{k}' are unit vectors along the initial and final relative momenta. Defining the triad of unit vectors

$$\begin{aligned} \hat{K} &= (\mathbf{k} - \mathbf{k}') / |\mathbf{k} - \mathbf{k}'| & \hat{P} &= (\mathbf{k} + \mathbf{k}') / |\mathbf{k} + \mathbf{k}'|, \\ \hat{n} &= (\mathbf{k} \times \mathbf{k}') / |\mathbf{k} \times \mathbf{k}'|, & \hat{K} \times \hat{P} &= \hat{n}, \end{aligned} \quad (1)$$

we have

$$C_{nn} = \langle \sigma_1 \cdot \hat{n} \sigma_2 \cdot \hat{n} \rangle, \quad (2)$$

and

$$C_{KP} = \langle \sigma_1 \cdot \hat{K} \sigma_2 \cdot \hat{P} \rangle.$$

These are the only nonvanishing correlation coefficients

* This work was supported by the Office of Naval Research.

† Now at Harvard University, Cambridge, Massachusetts.

‡ Now at University of Arizona, Tucson, Arizona.

§ Now at Purdue University, Lafayette, Indiana.

¹ M. H. MacGregor, M. J. Moravcsik, and H. P. Stapp, *Ann. Rev. Nucl. Sci.* **10**, 291 (1960).

² H. P. Stapp, M. J. Moravcsik, and H. P. Noyes, in *Proceedings of the 1960 Annual International Conference on High-Energy Physics at Rochester*, edited by E. C. G. Sudarshan, J. H. Tinlot, and A. C. Melissions (Interscience Publishers, Inc., New York, 1960), p. 128.

³ G. Breit, in *Proceedings of the 1960 Annual International Conference on High-Energy Physics at Rochester*, edited by E. C. G. Sudarshan, J. H. Tinlot, and A. C. Melissions (Interscience Publishers, Inc., New York, 1960), p. 132; G. Breit, M. H. Hull, Jr., K. E. Lassila, and K. D. Pyatt, Jr., *Phys. Rev.* **120**, 2227 (1960).

if the initial state is unpolarized. Figure 1(b) shows the laboratory configuration if relativistic corrections are ignored. The experiment thus consisted of measuring the simultaneous spin orientations of two protons after scattering. Neither the incident beam nor the target was polarized. The spin orientation measurement was performed by scattering the two protons in carbon and using the azimuthal asymmetry which results when a polarized proton scatters from a carbon nucleus. Spark chamber plates of $\frac{1}{2}$ -in.-thick graphite served as the polarization analyzer. The polar and azimuthal angles $\theta_1, \phi_1, \theta_2,$ and ϕ_2 of the resulting scatterings were measured from stereo photographs of the event.

The correlation coefficients can be expressed in terms of the joint distribution function

$$\begin{aligned} \frac{d^2\sigma}{d\Omega_1 d\Omega_2} &= \frac{d\sigma}{d\Omega_1} \frac{d\sigma}{d\Omega_2} [1 + P(\theta^*) P(\theta_1) \cos\phi_1 \\ &+ P(\theta^*) P(\theta_2) \cos\phi_2 + C_{nn} P(\theta_1) P(\theta_2) \cos\phi_1 \cos\phi_2 \\ &+ C_{KP} P(\theta_1) P(\theta_2) \sin\phi_1 \sin\phi_2]. \end{aligned} \quad (3)$$

$d\sigma/d\Omega_1$ and $d\sigma/d\Omega_2$ are the differential scattering cross sections in chambers 1 and 2 assuming the incident protons to be unpolarized. $P(\theta^*)$ is the polarization

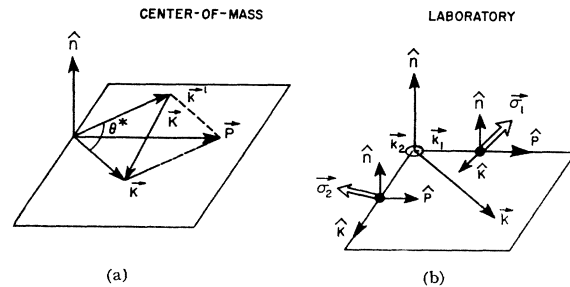
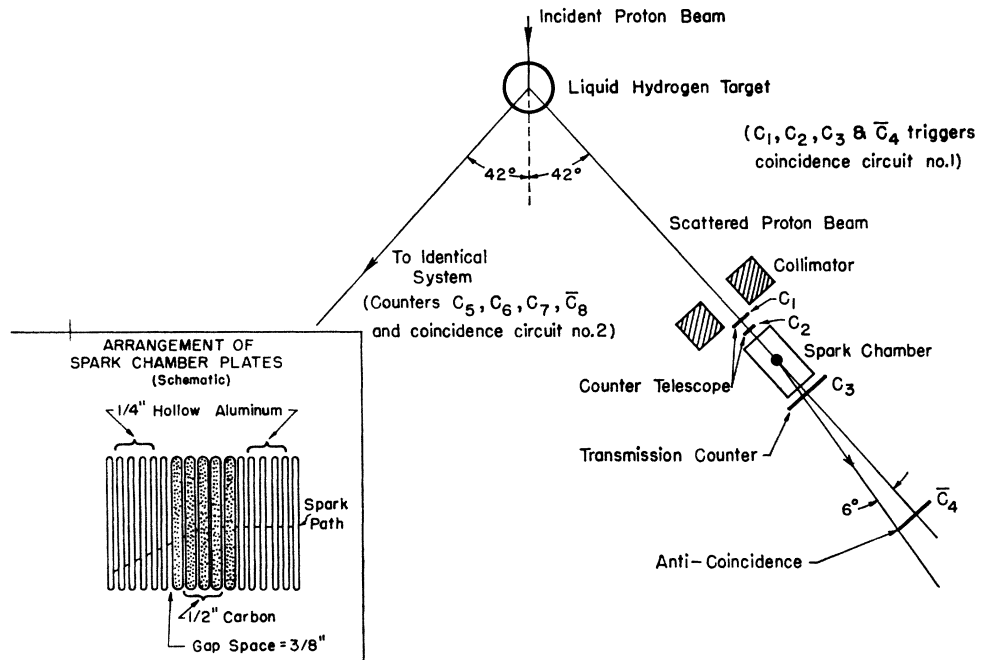


FIG. 1. (a) Unit vectors used in defining the correlation coefficients in the center-of-mass system. (b) Unit vectors from Fig. 1(a) transformed to the laboratory system assuming a nonrelativistic transformation for simplicity. \mathbf{k}_1 and \mathbf{k}_2 are the final proton momenta.

FIG. 2. The experimental geometry. The insert shows the arrangement of the carbon and the hollow aluminum plates.



acquired by an unpolarized proton beam scattering from hydrogen at the center-of-mass angle θ^* . $P(\theta_1)$ and $P(\theta_2)$ are the polarizations which an unpolarized proton at the appropriate incident energy would acquire when scattered from carbon at the laboratory angles θ_1 and θ_2 . At 90° in the center-of-mass system $P(\theta^*)=0$. Hence, at $\theta^*=90^\circ$ the joint distribution reduces to

$$\left. \frac{d^2\sigma}{d\Omega_1 d\Omega_2} \right|_{\theta^*=90^\circ} = \frac{d\sigma}{d\Omega_1} \frac{d\sigma}{d\Omega_2} [1 + C_{nn} P(\theta_1) P(\theta_2) \cos\phi_1 \cos\phi_2 + C_{KP} P(\theta_1) P(\theta_2) \sin\phi_1 \sin\phi_2]. \quad (4)$$

Expressions for C_{nn} and C_{KP} in terms of elements of the p - p scattering matrix at the energy and angle of interest may be found in reference 1. At $\theta^*=90^\circ$, the coefficient C_{nn} has a very simple form,

$$C_{nn} = 2t - 1; \quad (5)$$

where t is the fraction of triplet scattering. If there is no spin-flip scattering, $t(90^\circ)=0$, because all odd Legendre polynomials vanish at 90° .

II. EXPERIMENTAL PROCEDURE

The layout of the University of Chicago unpolarized 450-MeV external proton beam has been described elsewhere.⁴ For the 400-MeV runs, the beam was degraded by a lithium hydride absorber placed at the intermediate image point of the focusing magnets, 42 ft from the target. The beam was monitored by a secondary emission monitor.⁴ The beam energy was measured by range curves in copper. The full beam

energy was 449 ± 3 MeV, and the energy after the LiH absorber was inserted was 399 ± 3 MeV. The average beam intensity was 2×10^8 protons/sec with a 300 μ sec spill occurring 60 times a second. The beam spot at the position of the target had a diameter of approximately 1 in.

The hydrogen target cup was a cylinder 3 in. in diameter and 3 in. long, with its axis normal to the incident beam. The cup was made of 0.007-in. Mylar with stainless steel supports.

Figure 2 shows the experimental geometry. With the exception of the plate configuration of the chamber shown in the inset in Fig. 2, the spark chamber and optical system design was identical to the one described by Cronin.⁵ Five carbon plates were used at proton energies of 200 and 300 MeV incident on the chamber, and one carbon plate was used at 100 MeV. Each carbon plate was $\frac{1}{2}$ in. thick, and the gap spacing for all plates was $\frac{3}{8}$ in. The remainder of the plates were hollow aluminum frames $\frac{1}{4}$ in. thick with 0.003-in. aluminum foil stretched across both sides. The effective area of the chamber was 7-in. \times 7-in. Counters C_1 and C_2 were 2 in. \times 2 in. \times $\frac{1}{8}$ in. plastic scintillators, and counter C_2 was placed 10 ft from the center of the hydrogen target, subtending a full angle of 1° . Counter C_3 was 12 in. \times 12 in. \times $\frac{1}{8}$ in., and \bar{C}_4 , the anticoincidence counter, was a 12 in. diam, $\frac{1}{2}$ in. thick disk placed so as to subtend a half angle of 6° at the center of the spark chamber. Counters C_5 , C_6 , C_7 , and \bar{C}_8 formed an identical system with respect to the other spark

⁵ J. W. Cronin and G. Renninger, Proceedings of an International Conference on Instrumentation for High-Energy Physics, September, 1960, Lawrence Radiation Laboratory (unpublished), p. 271.

⁴ L. G. Pondrom, Phys. Rev. **114**, 1623 (1959).

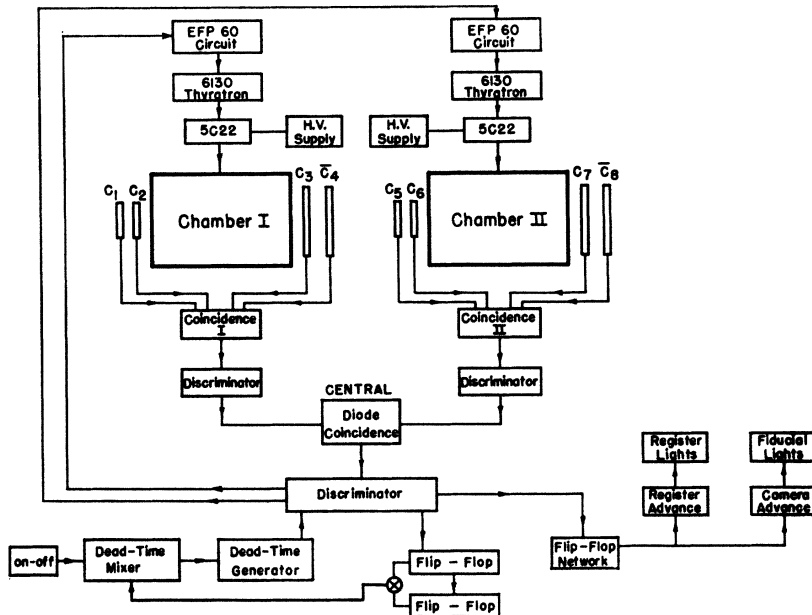


FIG. 3. Counter electronics and spark chamber logic.

chamber. The 42° - 42° configuration shown in Fig. 2 was used for the runs at 90° in the center of mass. Correlation data were taken by triggering the spark chambers on a p - p coincidence event in which both protons scattered sufficiently to miss the anticoincidence counters. The cameras were then advanced one frame, each register was advanced, and the fiducial and register lights were flashed. Care was taken to insure that the registers remained in step. A typical trigger rate for the system was two per second at a beam intensity of 2×10^9 protons/sec.

A block diagram of the electronics and spark chamber logic is shown in Fig. 3. Each 5C22 Thyatron discharged a $2500 \mu\mu\text{F}$ capacitor bank, 5 times the chamber capacity, at 15 kV across the plates of the chamber. The delay time between particle transversal and the discharge of the chamber was 250 nsec. The coincidence circuits and discriminators were of the Fitch type.⁶ The logic and coincidence circuitry was fully transistorized.

The only major correction to the values of the correlation coefficients obtained from the likelihood calculation is a correction due to accidentals, i.e., events which are interpreted by the electronics as having been a good p - p scatter but which actually consist of two protons that did not scatter from one another in the hydrogen target cup and consequently their spins cannot possibly be correlated. The corrected value for the coefficient C_{nn} is given by the expression:

$$C_{nn}^c = C_{nn}^u / (1 - \eta), \quad (6)$$

where η is the fraction of accidental events, C_{nn}^c is the corrected value of the coefficient, and C_{nn}^u is the un-

⁶ V. L. Fitch, in *Techniques of High Energy Physics*, edited by D. Ritson (Interscience Publishers, Inc., New York, 1961), p. 365.

corrected value obtained directly from the maximum likelihood calculation. A similar expression is used for C_{KP} .

The method of determining the fraction of accidental events consisted of inserting a length of delay cable (equal to a time corresponding to the reciprocal of the cyclotron radio frequency) between one of the coincidence circuits and the central diode coincidence circuit. Now there can be no correlated events because the central coincidence circuit is being triggered by pulses 50 nsec apart in time (see Fig. 3), yet the number of accidentals should be essentially unchanged. The fraction of accidental scatters for the 400 MeV, 90° and 60° experiments are 9% and 4%, respectively, and for the 450-MeV experiment the value of η is 14%.

The true background event rate, determined by counting correlated events with the target cup empty, was consistent with zero for all experiments. That the background rate is negligible is reasonable because the geometry of the experiment is sufficiently selective to eliminate events such as scatterings in the stainless steel.

III. ANALYSIS OF THE DATA

In order to apply Eqs. (3) and (4) to the observed spark chamber distributions, the effective carbon polarizations, $P(\theta_1)$ and $P(\theta_2)$ at the energies of interest must be known. For the $\theta^* = 90^\circ$ runs, these energies were 200 and 225 MeV for 400 and 450 MeV incident on the hydrogen target. The $\theta^* = 60^\circ$ run at 400 MeV was of course not symmetrical; the forward proton was at 300 MeV, and the backward one at 100 MeV. Because of the slow variation of the elastic polarization of carbon in the 200-MeV region, one calibration served for both 200 and 225 MeV. Calibrations at 200 and 100 MeV were performed using the 90% polarized proton

TABLE I. Average analyzing power of spark chamber vs proton kinetic energy.

Proton kinetic energy (MeV)	$P(\theta)_{av}$ (9° - 27°)
100	0.16 ± 0.02
200	0.50 ± 0.02
300	0.36 ± 0.07

beam at the University of Rochester cyclotron. The 300-MeV calibration was done with the 60% polarized beam at Chicago.

A typical 90° stereo photograph of a calibration run event is shown in Fig. 4. From the projected angles θ_s and θ_t in the side and top views, respectively, the polar angle θ and the azimuthal angle ϕ were calculated with the equations

$$\begin{aligned} \tan^2\theta &= \tan^2\theta_s + \tan^2\theta_t, \\ \cos\phi &= \tan\theta_t / \tan\theta, \\ \sin\phi &= \tan\theta_s / \tan\theta. \end{aligned} \quad (7)$$

Here a right-handed coordinate system is chosen, with the z axis along the incident proton direction, and the positive x axis to the left when viewed along positive z . The scanning criteria for an acceptable event were very simple. The incident proton was required to enter normally to within 1° ; the scatterer was required to take place in a carbon plate, and no extra sparks were permitted to leave the scattering vertex. This last requirement reduced the inelastic contamination. Figure 5 shows a plot of the 200-MeV calibration. Here θ was divided into 3° intervals from 9° to 27° , and $P(\theta)$ was calculated from the asymmetry $1 + \epsilon \cos\phi$, where

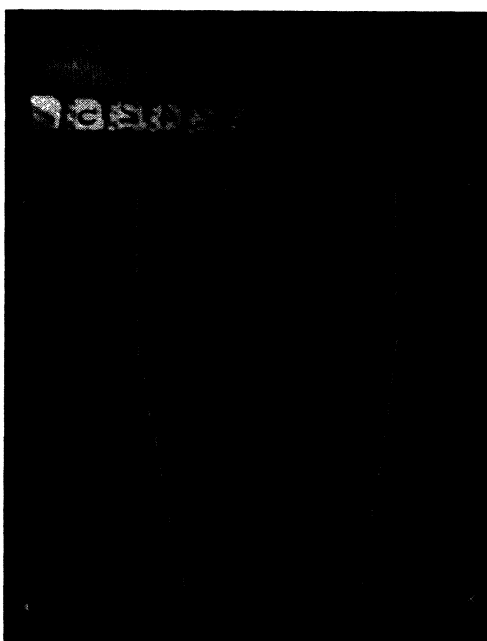


Fig. 4. Typical event showing two 90° stereo views of a proton scattering in a carbon plate. The crosses are fiducial marks.

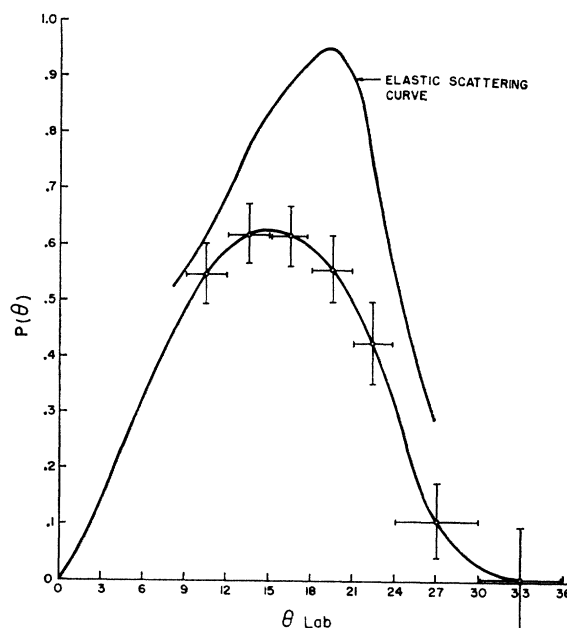


FIG. 5. Results of the 200-MeV calibration.

$\epsilon = P(\theta)P_B$, P_B being the beam polarization. The deviation of the curve from the expected pure elastic scattering is due to inelastic contamination which was eliminated neither by the scanning criteria nor by the counter selection. Table I gives the average analyzing power between 9° and 27° for the three proton energies.

The criteria for scanning the correlation data were the same as those applied to the calibration film. In this case, two pictures similar to Fig. 4 were measured for each event. If a second track appeared in either picture, the event was rejected. The measurement was done using an angle encoder manufactured by the Datex Corporation which had a least count of $\pm \frac{1}{3}^\circ$. The analysis of the data was done on an IBM-650 computer. Maximum likelihood calculations were performed by calculating the values of C_{nn} and C_{KP} which maximized the logarithm of L , where

$$L = \prod_{i=1}^N p_i, \quad (8)$$

and

$$\begin{aligned} p_i &= 1 + P(\theta^*)P(\theta_1^i) \cos\phi_1^i + P(\theta^*)P(\theta_2^i) \cos\phi_2^i \\ &\quad + C_{nn}P(\theta_1^i)P(\theta_2^i) \cos\phi_1^i \cos\phi_2^i \\ &\quad + C_{KP}P(\theta_1^i)P(\theta_2^i) \sin\phi_1^i \sin\phi_2^i. \end{aligned} \quad (9)$$

p_i is proportional to the probability for the i th event. For $\theta^* = 90^\circ$, the expression for p_i reduces to

$$p_i = 1 + C_{nn}x_i + C_{KP}y_i. \quad (10)$$

Since $|C_{nn}| \leq 1$ and $|C_{KP}| \leq 1$, and x_i, y_i are products of sines and cosines, one can expand the logarithm of

TABLE II. Summary of probability curves, accidental studies, and bias checks for the correlation coefficients.

	400 MeV $\theta^*=90^\circ$		400 MeV $\theta^*=60^\circ$		450 MeV $\theta^*=90^\circ$	
	C_{nn}	C_{KP}	C_{nn}	C_{KP}	C_{nn}	C_{KP}
Number of events	5797	5797	5800	5800	2463	2463
Uncorrected value from likelihood function	0.55 ± 0.086	0.29 ± 0.086	0.78 ± 0.43	0.57 ± 0.44	0.60 ± 0.14	0.32 ± 0.14
Accidentals	$(9 \pm 2)\%$	$(9 \pm 2)\%$	$(4 \pm 1)\%$	$(4 \pm 1)\%$	$(14 \pm 4)\%$	$(14 \pm 4)\%$
Instrumental correlation	$+0.04 \pm 0.05$	-0.05 ± 0.05	$+0.11 \pm 0.31$	$+0.08 \pm 0.33$	-0.03 ± 0.07	-0.08 ± 0.07
Uncertainty in analyzing power	4%	4%	13% (100 MeV) 20% (300 MeV)	13% (100 MeV) 20% (300 MeV)	4%	4%

L thus:

$$\ln L = C_{nn} \sum_{i=1}^N x_i + C_{KP} \sum_{i=1}^N y_i - \frac{1}{2} C_{nn}^2 \sum_{i=1}^N x_i^2 - C_{nn} C_{KP} \sum_{i=1}^N x_i y_i - \frac{1}{2} C_{KP}^2 \sum_{i=1}^N y_i^2 + \dots, \quad (11)$$

where N is the total number of events. From the projected angles measured for each event, θ_1 , ϕ_1 , θ_2 , and ϕ_2 were calculated and $P(\theta_1)$ and $P(\theta_2)$ were obtained by using the polynomial $P(\theta) = a + b\theta + c\theta^2$ which best fit the calibration curve in Fig. 5. With this information x_i and y_i were computed for each event i , and that combination of values of C_{nn} and C_{KP} which maximized L was taken as the best estimate of the

coefficients for the given data. Figure 6 shows a plot of the probability L as a function of C_{nn} for C_{KP} at its most probable value. The peak value of the curve is $C_{nn} = 0.55$, and the standard deviation is 0.086 for 5797 events. This uncorrected value was corrected for accidentals according to Eq. (6). The standard deviation on each result calculated by maximum likelihood is essentially equal to $\sigma \approx 2/N^{1/2} P_1 P_2$ where N is the total number of events and P_1 and P_2 are the appropriate average analyzing powers.

The spark chamber technique for correlation measurements offers an excellent check for instrumental biases because if there are N correlated events on the film, there are $N(N-1)$ uncorrelated events. In fact, each event i in one chamber was correlated with its nearest neighbors $i \pm 1$, and second nearest neighbors, $i \pm 2$ to check for biases. Table II summarizes the results of the data calculations, accidentals corrections, and correlated bias checks for all correlation coefficients. Table III gives the final values for the coefficients. The

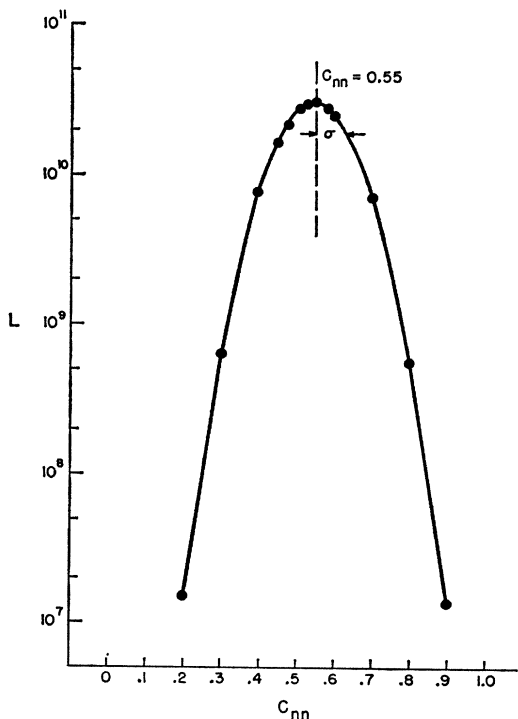


FIG. 6. A section of the three-dimensional likelihood surface along the C_{nn} direction assuming the peak value for C_{KP} .

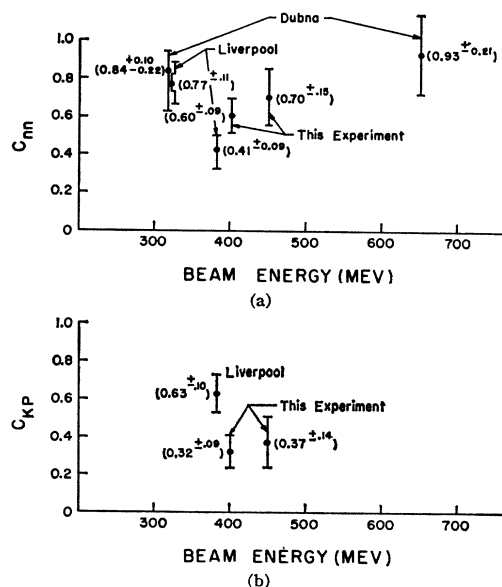
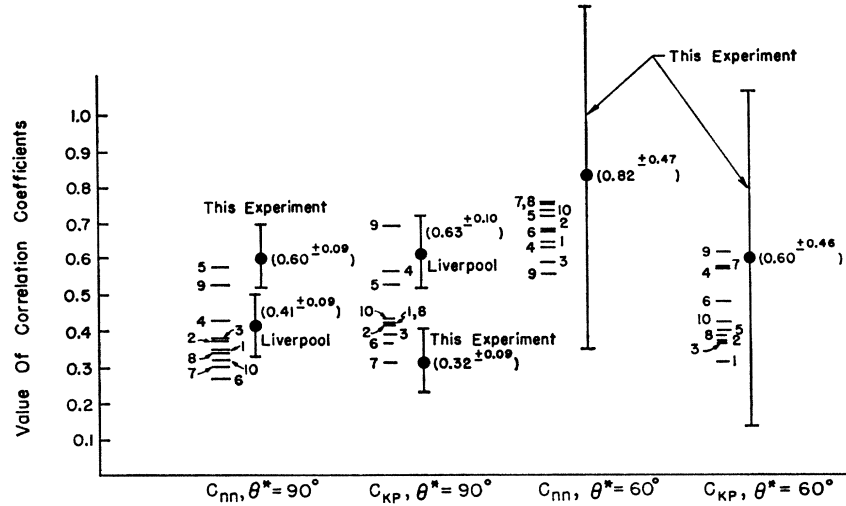


FIG. 7. Correlation coefficient measurements for p - p scattering at 90° in the center-of-mass system. The Liverpool data are discussed in references 7, 8, and 9, while the Dubna points are discussed in 10 and 11.

FIG. 8. A comparison of the present data with predicted values of Moravcsik.



errors in the 60° values are very large because the analyzing powers given by Table I are comparatively small.

IV. DISCUSSION

Figure 7 summarizes all of the correlation coefficients⁷⁻¹¹ at 90° in the center of mass which have been measured to date. C_{nn} is large and positive from 310 to 650 MeV, which implies a large fraction of spin-flip scattering, as indicated by Eq. (3). Since an abrupt phase-shift change between 382 and 400 MeV is not expected, a discrepancy seems to exist between the Liverpool measurements and the present data. The 382-MeV C_{nn} is 2 standard deviations below the present 400-MeV result, and the 382-MeV C_{KP} value is 3 standard deviations above the present point. A benefit of the spark chamber technique is that C_{nn} and C_{KP} are measured simultaneously, and any systematic error other than scanning bias should effect both values in the same way. Scanning biases were checked by the nearest-neighbor correlation.

TABLE III. Final values of the correlation coefficients.

	400 MeV, $\theta^*=90^\circ$	400 MeV, $\theta^*=60^\circ$	450 MeV, $\theta^*=90^\circ$
C_{nn}	0.60 ± 0.09	0.82 ± 0.47	0.70 ± 0.15
C_{KP}	0.32 ± 0.09	0.60 ± 0.46	0.37 ± 0.14

⁷ J. V. Allaby, A. Ashmore, A. N. Diddens, and J. Eades, Proc. Phys. Soc. (London) **74**, 482 (1959).

⁸ A. Ashmore, A. N. Diddens, and G. B. Huxtable, Proc. Phys. Soc. (London) **73**, 957 (1959).

⁹ A. Ashmore, A. N. Diddens, G. B. Huxtable, and K. Skarsvåg, Proc. Phys. Soc. (London) **72**, 289 (1958).

¹⁰ I. M. Vasilevskii, V. V. Vishnyakov, E. I. Ilescu and A. A. Tyapkin, J. Exptl. Theoret. Phys. (U.S.S.R.) **39**, 889 (1960) [translation: Soviet Phys.—JETP **12**, 616 (1961)].

¹¹ V. P. Dzhelepov, in *Proceedings of the 1960 Annual International Conference on High-Energy Physics at Rochester*, edited by E. C. G. Sudarshan, J. H. Tinlot, and A. C. Melissios (Interscience Publishers, Inc., New York, 1960), p. 115.

Stapp, Moravcsik, and Noyes have recently expressed the phase shifts as smooth functions of energy, and have extrapolated the phase shifts to 400 MeV. Ten sets of phase shifts gave good χ^2 fits to the data between 310 and 382 MeV.¹² The Liverpool correlation coefficients were included in the extrapolation. Figure 8 gives the present results for C_{nn} and C_{KP} at $\theta^*=90^\circ$ and 60° at 400 MeV, and also the predicted values given by the ten extrapolated solutions. In order to compare the predictions with the experiment, the predicted values of C_{KP} have been corrected for relativistic effects according to the prescription of Sprung.¹³ C_{nn} involves spin components normal to the direction of the Lorentz transformation, and hence suffers no correction. The present results are unable to choose between the 10 phase shift fits at 400 MeV. That qualitative agreement exists is not surprising, since the Liverpool data were used in the extrapolation, and we agree qualitatively with their points. If our data were included in the extrapolated fit, the predictions would be changed somewhat. In particular C_{KP} at 90° would be brought down. Because of their large errors, the 60° data would have little effect. A unique solution, however, would not be expected. A complete set of p - p triple scattering data from spark chambers has been obtained on film, and an analysis of the data is now in progress. It is hoped that these results will clear up ambiguities in the phase-shift analysis at 400 MeV.

ACKNOWLEDGMENTS

The authors take great pleasure in thanking their many colleagues for their untiring work in carrying this experiment to its conclusion. The liquid hydrogen target was designed by Max Scheibner who also supervised its construction. Mrs. D. Josephine Elms is credited with having done many of the computations

¹² M. J. Moravcsik (private communication).

¹³ D. W. L. Sprung, Phys. Rev. **121**, 925 (1961).

associated with the analysis. In addition, she and her scanning staff are to be thanked for having successfully completed a formidable scanning assignment.

Finally, the authors wish to thank Dr. Michael Moravcsik for many valuable communications, Professor George T. Reynolds for having made available

the facilities of the Elementary Particles Laboratory, Professor John H. Tinlot for providing the staff and facilities of the University of Rochester cyclotron and Professor Herbert L. Anderson for providing the facilities and staff of the University of Chicago cyclotron.

Possible Determination of the Spin of the Ξ^- from the Angular Asymmetry of Its Decay*

MURRAY PESHKIN

Argonne National Laboratory, Argonne, Illinois

(Received 1 October 1962)

The Ξ^- hyperon is produced in a parity-conserving interaction involving only a proton and two spinless K mesons. Therefore, the Ξ^- beam in any direction consists of an equal, incoherent mixture of two pure spin states which go into each other under 180° rotation in the production plane. This condition implies a new restriction upon the angular distribution of the Ξ^- decay products. In particular, the distribution $I(\theta, \phi) = 1 + A \cos\theta$ is impossible for $A \neq 0$ unless the Ξ^- spin is $\frac{1}{2}$.

1. INTRODUCTION

RECENT experiments¹ suggest the possibility that the usual methods of analyzing angular distributions in the decay of the Ξ^- hyperon may not be able to distinguish between spin $\frac{1}{2}$ and spin $\frac{3}{2}$ for the hyperon. In these experiments, the hyperon is produced in one of the reactions

$$K^- + p \rightarrow \Xi^- + K^+, \quad (1.1)$$

$$K^- + p \rightarrow \Xi^- + K + \pi, \quad (1.2)$$

and subsequently decays according to

$$\Xi^- \rightarrow \Lambda^0 + \pi^-. \quad (1.3)$$

The method of Adair² suffers from the paucity of Ξ^- production events wherein all particles move nearly along the line of the incident K^- beam. The method of Lee and Yang³ applies to all Ξ^- directions. However, it results at best in a series of inequalities which cannot exclude Ξ^- spin J unless the measured decay asymmetry satisfies

$$|\langle \cos\theta \rangle| > 1/6J \quad (1.4)$$

for some production direction of the Ξ^- . The polar angle θ in relation (1.4) is that formed by the momentum of the decay pion, in the rest system of the hyperon. The polar (z) axis is perpendicular to the plane con-

taining the momenta of the Ξ^- and the incident K^- . This method of analysis involves no assumptions about the production process, and is therefore incapable of making effective use of the azimuthal angular distribution in decay.

The asymmetry theorems of Peshkin⁴ also fail to decide between the possible spins of $\frac{1}{2}$ and $\frac{3}{2}$ for the Ξ^- . The failure here is due to discarding the information contained in the odd part of the angular distribution in parity-mixing decay.

The discussion below extends the second asymmetry theorem of reference 4 to cover decay of Ξ^- hyperons produced in reaction (1.1). The argument makes use of the zero spin of the K meson and of parity conservation in the production process. The result is an unambiguous test between spin $\frac{1}{2}$ and spin $\frac{3}{2}$, provided that the decay gives some evidence of parity mixing, and that the decay angular distributions are measured with sufficient accuracy. Thus the right-hand side of inequality (1.4) is replaced by zero.

2. ASYMMETRY CONDITIONS

In reaction (1.1), the initial beam consists of an equal, incoherent mixture of two pure quantum states. In one state the proton spin is parallel to the K^- momentum; in the other it is antiparallel. These two states go into each other under the symmetry operation which consists of space inversion followed by 180° rotation about the normal to the production plane. Under the same symmetry operation, the momentum of the Ξ^- goes into itself. Therefore the Ξ^- "beam" in a given direction consists of an equal, incoherent mixture

* Work performed under the auspices of the U. S. Atomic Energy Commission.

¹ L. Bertanza, V. Brisson, P. L. Connolly, E. L. Hart, I. S. Mitra, G. C. Moneti, R. R. Rau, N. P. Samios, I. O. Skillicorn, S. S. Yamamoto, M. Goldberg, L. Gray, J. Leitner, S. Lichtman, and J. Westgard, Phys. Rev. Letters 9, 229 (1962).

² R. K. Adair, Phys. Rev. 100, 1540 (1955).

³ T. D. Lee and C. N. Yang, Phys. Rev. 109, 1755 (1958).

⁴ M. Peshkin, Phys. Rev. 123, 637 (1961).

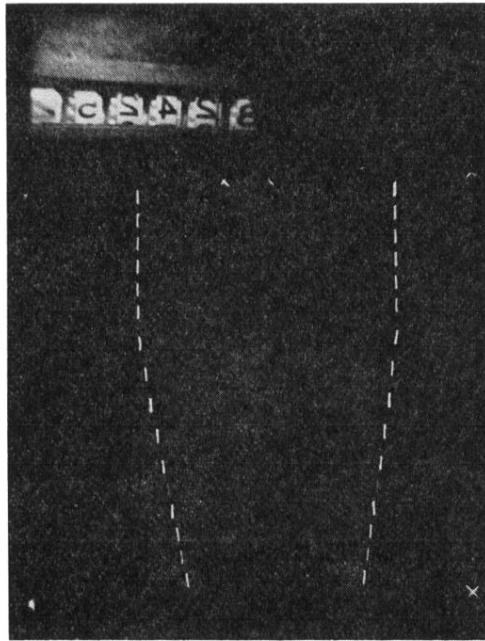


FIG. 4. Typical event showing two 90° stereo views of a proton scattering in a carbon plate. The crosses are fiducial marks.